Materials Science and Engineering C 49 (2015) 761–768

Contents lists available at ScienceDirect

Materials Science and Engineering C

journal homepage: www.elsevier.com/locate/msec

Surface characterization and cytotoxicity response of biodegradable magnesium alloys

Luis Pompa, Zia Ur Rahman, Edgar Munoz, Waseem Haider *

Mechanical Engineering Department, University of Texas Pan American, Edinburg, TX, United States

ARTICLE INFO

Article history:
Received 22 April 2014
Received in revised form 6 December 2014
Accepted 5 January 2015
Available online 8 January 2015

Keywords:
Magnesium
Corrosion
Biodegradable
Cytotoxicity
Surface treatment

ABSTRACT

Magnesium alloys have raised an immense amount of interest to many researchers because of their evolution as a new kind of third generation materials. Due to their biocompatibility, density, and mechanical properties, magnesium alloys are frequently reported as prospective biodegradable implant materials. Moreover, magnesium alloys experience a natural phenomenon to biodegrade in aqueous solutions due to its corrosion activity, which is excellent for orthopedic and cardiovascular applications. However, a major concern with such alloys is fast and non-uniform corrosion degradation. Controlling the degradation rate in the physiological environment determines the success of biodegradable implants. In this investigation, three different grades of magnesium alloys: AZ31B, AZ91E and ZK60A were studied for their corrosion resistance and biocompatibility. Scanning electron microscopy, energy dispersive spectroscopy, atomic force microscopy and contact angle meter are used to study surface morphology, chemistry, roughness and wettability, respectively. Additionally, the cytotoxicity of the leached metal ions was evaluated by using a tetrazolium based bio-assay, MTS.

1. Introduction

Biological implants have been used in many different applications today, such as orthopedic and cardiovascular. Typical biomaterials encompass stainless steel alloys, cobalt-chrome alloys, titanium alloys, alumina, zirconia, poly-methyl-methacrylate (PMMA), poly-lactic acid (PLA), etc. Most of the biomedical devices made from these materials are designed to stay permanently in the body. However, it has been reported that long-term implantations lead to complications, including sensitizations and allergies. There is also a need for secondary surgery to remove implants which may increase health care cost and mortality rates [1]. To overcome these limitations associated with permanent implant materials, biodegradable materials are proposed. Biodegradable magnesium alloys are considered potential materials for the fabrication of medical implants. Magnesium possesses an important property such as biodegradability; characteristic of the material to degrade in a biological environment such as the human body [2]. Magnesium alloys are considered an alternative material useful for the fabrication of cardiovascular, orthopedic and trauma stomach devices [3–7]. Magnesium alloys have similar density and Young's modulus as bones (E = 40–45 GPa for Mg and E = 3–20 GPa for bone) [8]. Even the strength/density ratio is greater than stainless and titanium alloys [9]. Moreover, magnesium is the fourth most abundant cation in the human body, with an estimation of 1 mol of magnesium in a normal 70 kg adult [2]. Magnesium serves as co-factor for many enzymes and delivers functions as a stabilizer for DNA and RNA structures [2,10]. Magnesium can even accelerate bone tissue growth [11]. However, it is important to take into consideration that high rate of magnesium alloy ions and particles released from an implant in the human body can be toxic. The high concentration of metal ions such as zirconium, aluminum, and rare earth metals produced through the corrosion activity may lead to harmful diseases inflammatory cascades and tissue damage [2,12–15]. High aluminum concentration is also harmful to neurons and osteoblasts and may cause dementia and Alzheimer's disease [16,17].

A major drawback with magnesium is its corrosion resistance. Most of the time such inadequate characteristic has deferred its wide scale use in many applications. Magnesium alloys corrode in aqueous solutions, and the different oxidation–reduction reactions are affected by the different alloying elements. Typically, the corrosion of magnesium will produce hydrogen gas and magnesium hydroxide. The following are the common anodic, cathodic and net reactions [18]:

$$\text{Anodic} \qquad Mg \rightarrow Mg^{2+} + 2e^{-} \tag{1}$$

$$\text{Cathodic} \qquad 2H_2O + 2e^{-} \rightarrow H_2 + 2(OH^{-}) \tag{2}$$

$$\text{Net reaction} \qquad Mg + 2H_2O \rightarrow Mg(OH)_2 + H_2. \tag{3}$$

Previous works [11,19–22] reported that organic and inorganic components could influence the corrosion rate of magnesium alloys. Due to this corrosion activity, the mechanical integrity can be affected before

* Corresponding author.
E-mail address: haiderw@utpa.edu (W. Haider).

http://dx.doi.org/10.1016/j.msec.2015.01.017
0928-4931/

Table 1
Chemical composition of PBS solution (g/l).

NaCl	Na_2HPO_4	$NaHCO_3$	KCl	KH_2PO_4	$MgSiO_4$	$CaCl_2$
8.0	0.06	0.35	0.4	0.06	0.2	0.14

certain tissues heal without any negative effects e.g., hard-tissue implantation repairs may require at least 12 weeks [2].

The process of alloying elements with magnesium leads to an improvement in both corrosion resistance and corrosion rate of magnesium [20,23]. It is reported that addition of aluminum into magnesium increases the ductility, yield strength and ultimate tensile strength via the formation of β-Mg_{17}-Al_{12} phase [17,24]. Similarly, the addition of zinc into magnesium improves corrosion resistance, creep behavior, yield strength and tensile strength of the alloy when the Zn content is less than 6 wt.% [24,25]. Decrease in elongation and tensile strength takes place when Zn content is over 6 wt.% [10]. Zn can also encumber the movement of the recrystallized grain boundary to refine the microstructure [17]. The addition of zirconium to magnesium enhances grain refinement. However, zirconium cannot be used with Mg containing aluminum because it can be removed from solid solution due to the formation of stable compounds [26].

Surface modifications are known to significantly improve surface properties of magnesium alloys. Since magnesium alloys are considered biodegradable alloys, they can only receive certain types of surface modifications. These types of surface treatments are chosen according to the environment the implant will be placed in [27]. Anodization is an electrochemical treatment that changes the surface chemistry of the metal by oxidation, producing a stable oxide layer. A thin layer at the metal-oxide interface, followed by a less dense porous oxide layer, characterizes the structure of the oxide film [28]. The anodizing behavior is strongly influenced by the voltage, current, temperature, and

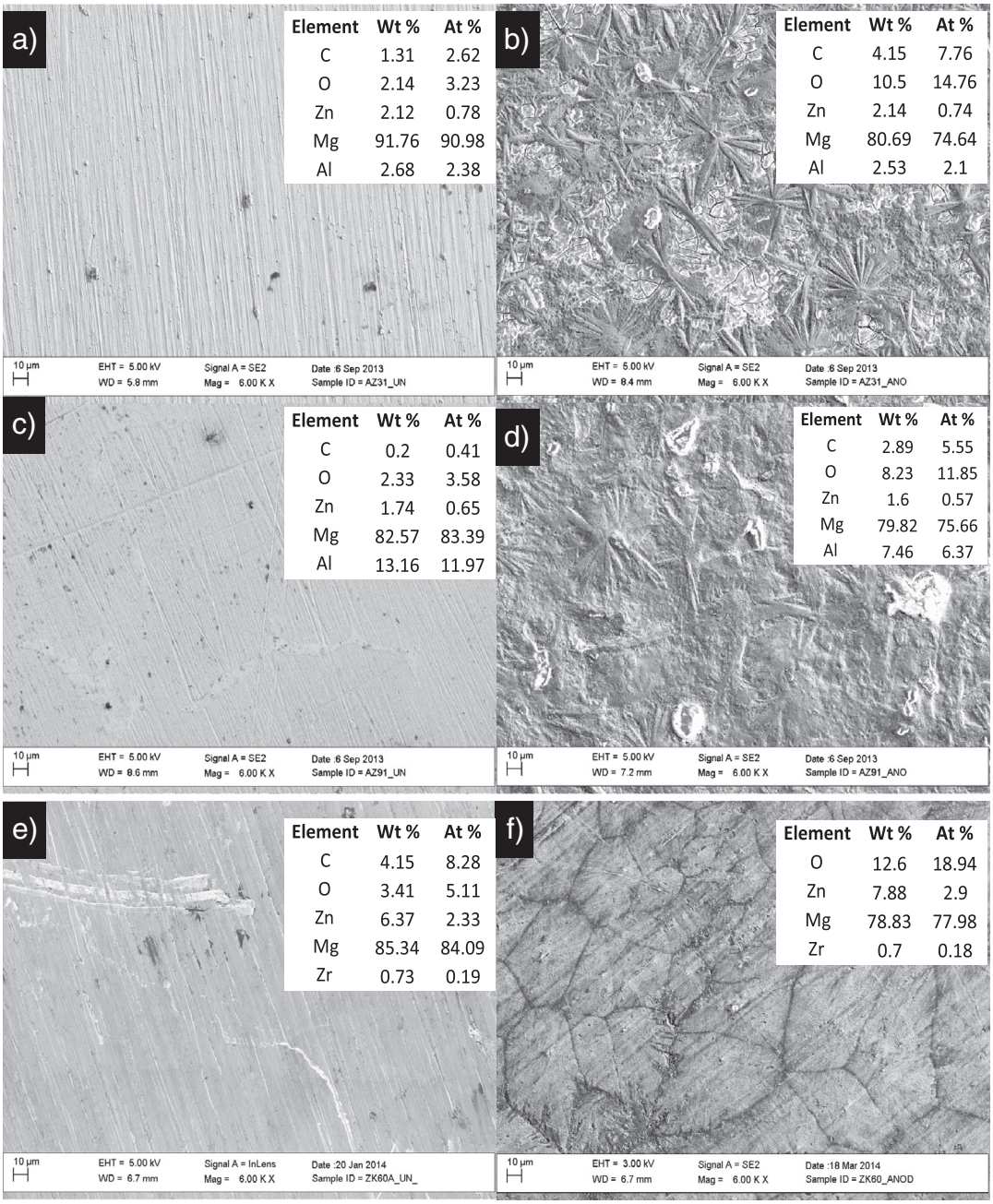

Fig. 1. SEM images of magnesium alloys: a) AZ31B untreated b) AZ31B anodized, c) AZ91E untreated, d) AZ91E anodized, e) ZK60A untreated f) ZK60A anodized.

concentration of electrolyte [28,29]. Anodization can increase the film thickness, biocompatibility, corrosion resistance, hardness, resistance to wear, and can even influence adhesion properties [30,31].

2. Experimental

2.1. Materials and methods

The specimens were made of AZ31B (3.0 wt.% Al, 1.0 wt.% Zn, Mg balance), AZ91E (9.0 wt.% Al, 1.0 wt.% Zn, Mg balance) and ZK60A (6.0 wt.% Zn, 0.45 wt.% Zr, Mg balance) magnesium alloys. The alloys were received in the form of rods and were cut into small disks with dimensions: 19 mm diameter and 4 mm thickness. Each sample was mechanically ground up to 1200-grit SiC paper, ultrasonically cleaned and degreased using ethanol and then air-dried. Magnesium alloys were anodized by Electrobright®(Macungie, PA, USA). Briefly, magnesium samples were subjected to anodization using a proprietary electrolyte consisting of a mixture of alcohol and organic acid at a constant voltage of 20 V, temperature of 10 °C for 30 min, using tungsten (W) as the cathode material.

2.2. Material characterization

The surface morphology of the specimens was analyzed by scanning electron microscopy (Sigma VP Carl Zeiss, Germany). The element distribution on the surface of the alloys was investigated by energy dispersive spectroscopy (EDS) (Carl Zeiss, Germany). The surface roughness was analyzed (20 × 20 μm area) by atomic force microscopy (Nanoscope IV MultiMode in air, Digital Instruments, Santa Barbara, CA, USA). The contact angle, surface free energy and work of adhesion were measured by applying the sessile drop method using the Kyowa angle meter (DM-CE1 Japan).

2.3. Electrochemical analysis

Electrochemical measurements were performed utilizing a standard three-electrode corrosion cell employing a GAMRY potentiostat (reference 600) with saturated calomel electrode as the reference, a graphite bar as the counter electrode, and magnesium alloy samples as working electrodes (1 cm^2 area exposed). The potentiodynamic polarization scans were carried out in accordance with ASTM: G102-89 [32]. The scanning rate was 1 mV/s. The temperature was kept at 37 °C using phosphate buffer saline as the electrolyte (pH 7.2–7.4), the PBS composition is found in Table 1.

2.4. Cytotoxicity assessments

The effect of metal ions released from magnesium alloys was assessed by using MTS assay (G3580, Celltiter 96®AQ_{ueous}One Solution Reagent, Promega Corporation) to determine the percentage of viable MC3T3-E1 (ATCC® CRL-2A593™) cells in extract solutions exposed to different concentrations. The cells were cultured in MEM alpha modification media (Thermo Scientific™ HyClone™ SH3026501), 10% fetal bovine serum, FBS, (Thermo Scientific™ HyClone™ SH3008803HI), and

Table 2
Surface characterization properties of Mg alloys.

Mg alloys	3-Dimensional optical image of alloy surface (20 × 20 μm)	Average surface roughness (nm) n = 3	Average contact angle (°) — DI water, ethylene glycol, diiodomethane (acid–base theory) n = 10	Surface free energy (mJ/m^2) (acid–base) n = 10
AZ31B untreated	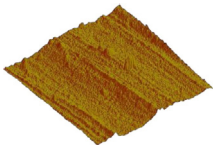	48.58 ± 23.45	58.72 ± 0.46 44.84 ± 0.28 40.16 ± 0.18	39.52 ± 0.09
AZ31B anodized	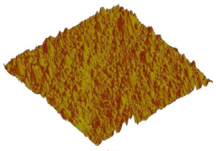	48.96 ± 10.23	98.41 ± 0.51 71.49 ± 0.88 66.86 ± 0.13	25.67 ± 0.12
AZ91E untreated	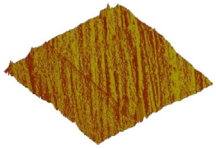	29.76 ± 12.69	62.98 ± 0.42 47.85 ± 0.23 41.82 ± 0.06	38.69 ± 0.03
AZ91E anodized	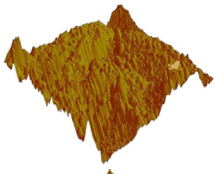	204.81 ± 62.70	93.36 ± 0.84 67.29 ± 0.28 51.15 ± 0.23	33.63 ± 0.13
ZK60A untreated	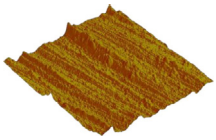	78.30 ± 21.63	67.16 ± 0.34 50.83 ± 0.13 43.42 ± 0.10	37.84 ± 0.05
ZK60A anodized	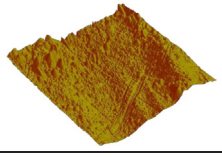	75.88 ± 34.49	72.05 ± 0.60 53.59 ± 0.26 44.16 ± 0.13	37.47 ± 0.07

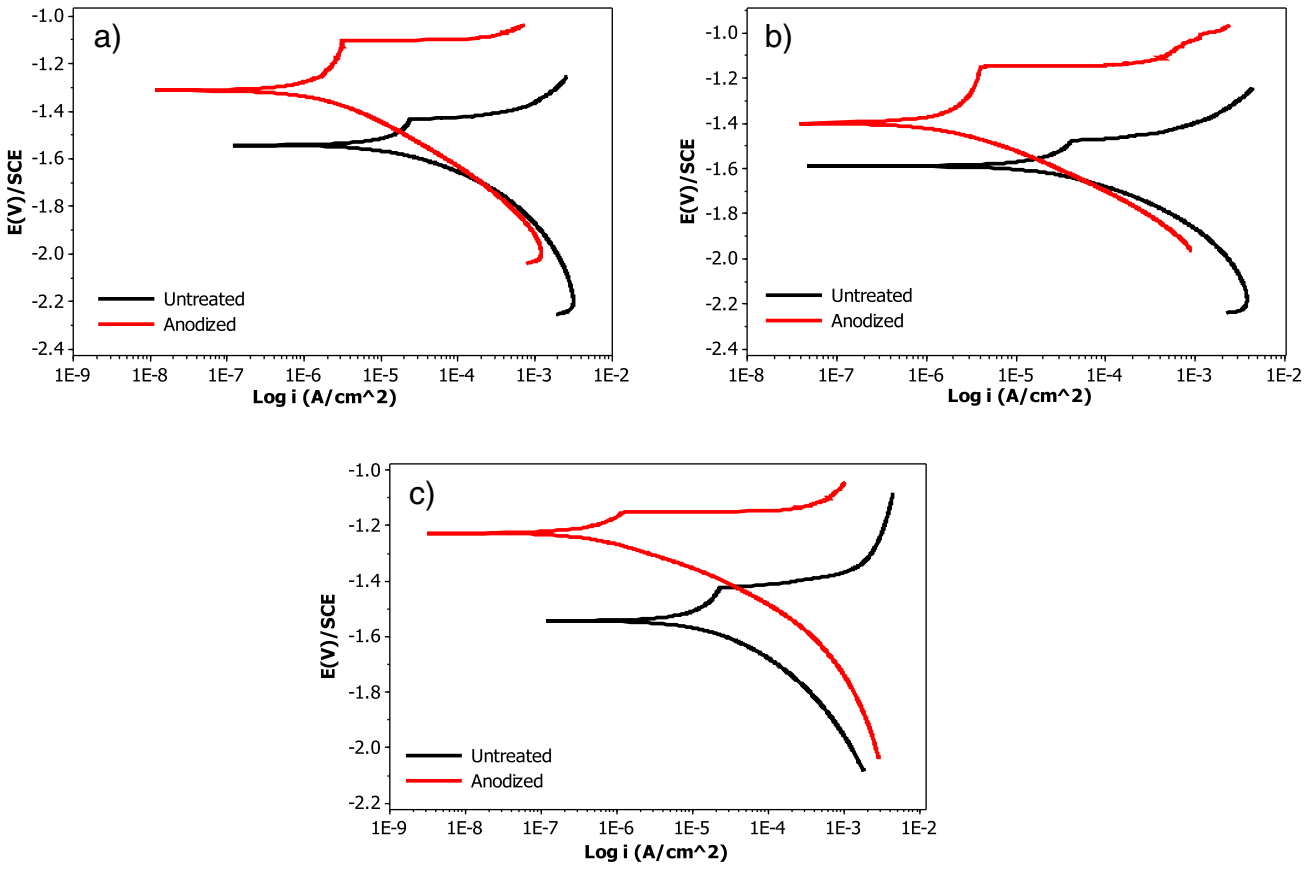

Fig. 2. Potentiodynamic polarization curves of magnesium alloys: a) AZ31B, b) AZ91E, and ZK60A.

Penicillin–Streptomycin (Sigma-Aldrich P4333) at 37 °C in a humidified atmosphere having 5% CO_2. The AZ31B, AZ91E, and ZK60 mg alloys were immersed in MEM alpha modification media for 21 days, and the media was changed and collected after every 3 days. Cells were counted (2×10^4 cells) using hemocytometer and plated in 96-well plates with 200 μl of culture media per well. The cells were incubated for 24 h to allow attachment. After the 24-hour incubation, the culture media was replaced with culture media exposed to magnesium alloys (100% concentrations). Pure culture media with cells was used as control. The cells were incubated for 24 h. After the 24 h, 100 μl of media were removed from the 96-well plates, the remaining 100 μl media was treated with 20 μl/well with Celltiter 96® AQ_{ueous} One Solution Reagent. The 96-well plates were placed in the incubator for 4 h. Immediately after the incubation period, the optical density measurements were recorded using ELx800™ BioTek absorbance microplate reader controlled by Gen5 software with a 490 nm absorbance excitation filter. Statistical analysis was executed to evaluate the difference in cell viability by the analysis of variance. One-way ANOVA was used to determine the significance of pairwise comparisons. Differences were considered statically significant ($P < 0.05$) and not significant ($P > 0.05$).

3. Results and discussion

3.1. Surface morphology and chemistry

Fig. 1 presents the surface morphologies and elemental surface distribution information of magnesium alloys. Different surface morphologies were observed before and after the anodization treatment. Fig. 1a,c and e exhibit untreated alloys with typical grinding marks. On the other hand, Fig. 1b,d and f shows anodized magnesium alloys with micro-textured morphologies. The anodization treatment produced an oxide film, which is intended to improve the corrosion resistance [33]. The anodized morphologies demonstrate some micro-texture patterns throughout the treated surface for AZ31 and AZ91, however ZK60 morphology shows the grain boundaries of the alloy. Furthermore, the EDS demonstrated the surface composition for each of the alloys. The increased oxygen content was observed for anodized samples when compared to untreated samples. High oxygen concentration indicates that the anodic film is made up of magnesium oxides and hydroxides [34]. There are different factors that can influence the behavior of the anodized films formed on magnesium alloys. For instance, intermetallic compounds, grain boundaries, cavities, small and large voids can have an effect on the anodic layer [30]. Similarly, the differences in micro-textured films (Fig. 1b,d & f) largely depends on the surface structure of the cast material [30]. Moreover, dielectric breakdown may cause spark discharge and gas generation at the time of the film formation. This event can also influence the structure of the film as shown in the SEM micrographs. Some of the cracks that appear on Fig. 1b might be the result of the internal stress when film is being formed [30,35]. Fig. 1d depicts a smoother appearance and this might be due to the higher aluminum content in the Mg alloy [36].

Table 3
Average electrochemical results with standard deviations of potentiodynamic polarization of Mg Alloys (n = 3).

Alloy	I_{corr} (A/cm^2) E−06	E_{corr} (V)	C.R. (mpy)
AZ31 untreated	34.5 ± 3.5	−1.54 ± 0.01	29.98 ± 2.5
AZ31 anodized	2.72 ± 0.8	−1.31 ± 0.03	2.36 ± 0.4
AZ91 untreated	36.6 ± 3.2	−1.59 ± 0.02	30.85 ± 2.8
AZ91 anodized	2.50 ± 0.5	−1.40 ± 0.06	2.11 ± 0.3
ZK60 untreated	32.3 ± 2.6	−1.55 ± 0.05	26.75 ± 0.5
Zk60 anodized	1.86 ± 0.2	−1.25 ± 0.01	1.54 ± 0.3

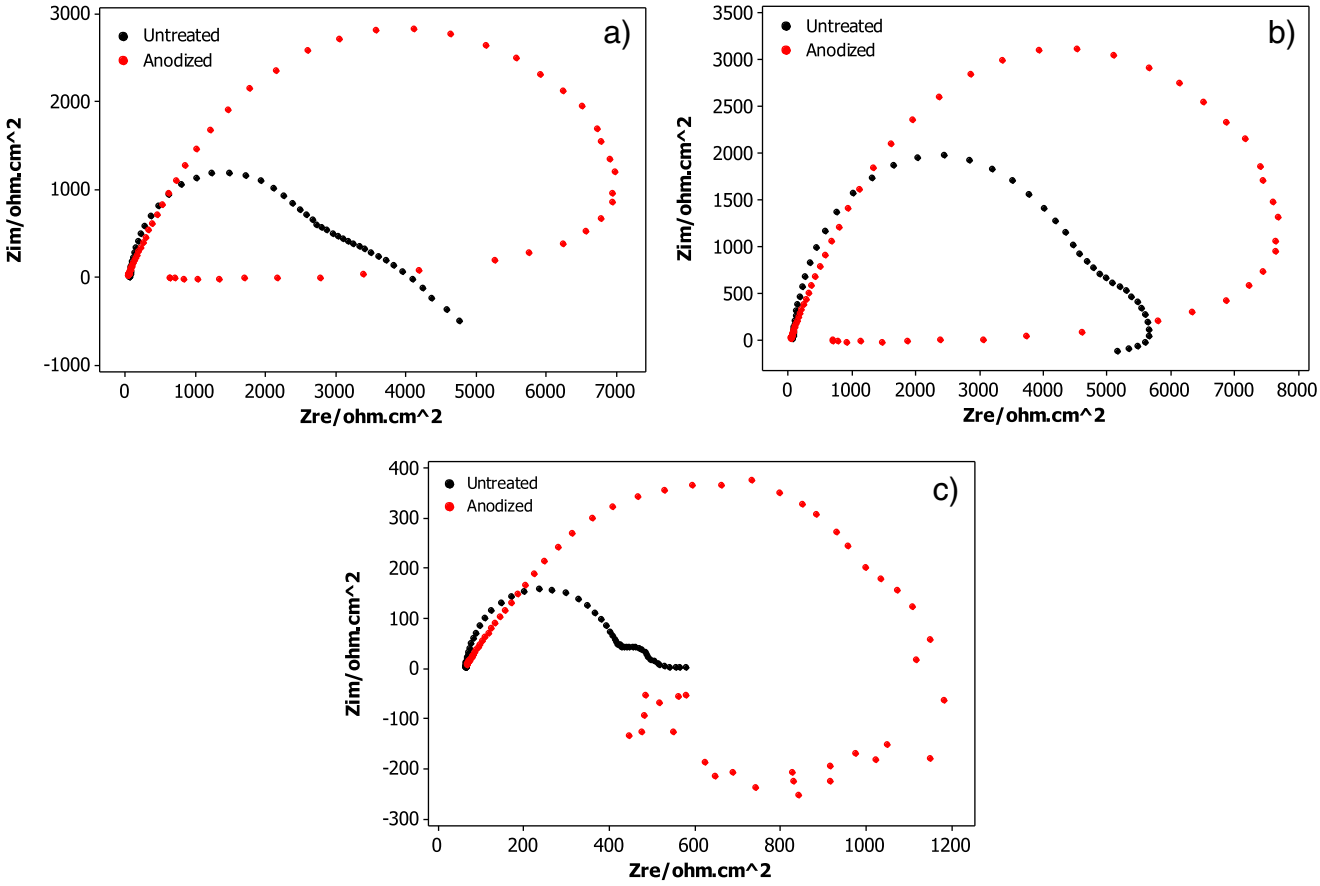

Fig. 3. Nyquist plots of magnesium alloys: a) AZ31B, b) AZ91E, and c) ZK60A.

3.2. Surface roughness and wettability

In this investigation, surface roughness and wettability has been studied. Table 2 shows the surface properties of magnesium alloys. The average surface roughness (R_a) and standard deviation was calculated and recorded for all untreated and anodized alloys. The results for the AZ31B and ZK60A alloys did not have any significant change in the surface roughness. However, for the AZ91E alloys, R_a values increased for the anodized alloys. AZ91E untreated alloys showed the lowest surface roughness, while the highest roughness was measured for AZ91E anodized alloys. The surface roughness is partly related to non-homogeneity of anodic layer and the formation of pores and cracks on the anodic film. These defects were greater in case of AZ91E when compare to AZ31B and ZK60A alloys [37]. Rough surfaces exhibit more surface area and reveal a better bone integration via the osseointegration process. Interaction between tissues and implants surfaces is typically controlled by

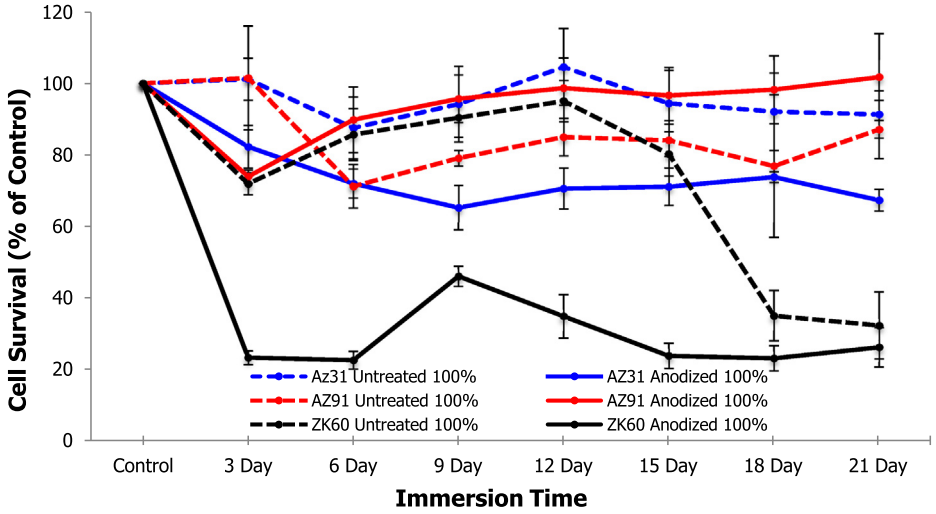

Fig. 4. Effect of Mg Alloys on MC3T3 cells after 1-day incubation.

the finish and texture of the implant material. Similarly, micro-textured surface (Fig. 1b,d and f) characteristics allow in growth of the tissues [38,39].

Contact angle measurements provide information on the wettability properties of a biomaterial. Wettability can influence protein absorption and cell activity. In this investigation, wettability results have shown that the contact angle increases (hydrophobic behavior) with the three liquid probes for the anodized alloys. On other hand, the surface free energy is lower for the anodized alloys when compared with untreated alloys.

3.3. Electrochemical analysis

The electrochemical polarization curves from the different magnesium alloys immersed in PBS are shown in Fig. 2. Three samples of each type of magnesium alloy ($n = 3$) were used in the analysis. In theory, the cathodic curve represents the hydrogen evolution through the reduction process, while the anode curve characterizes the oxidation of Mg. Longest passivation stages were observed for AZ31B and AZ91E anodized compared to ZK60A anodized passivation area. The corrosion potential E_{corr}, the current density I_{corr}, and corrosion rate C.R. results

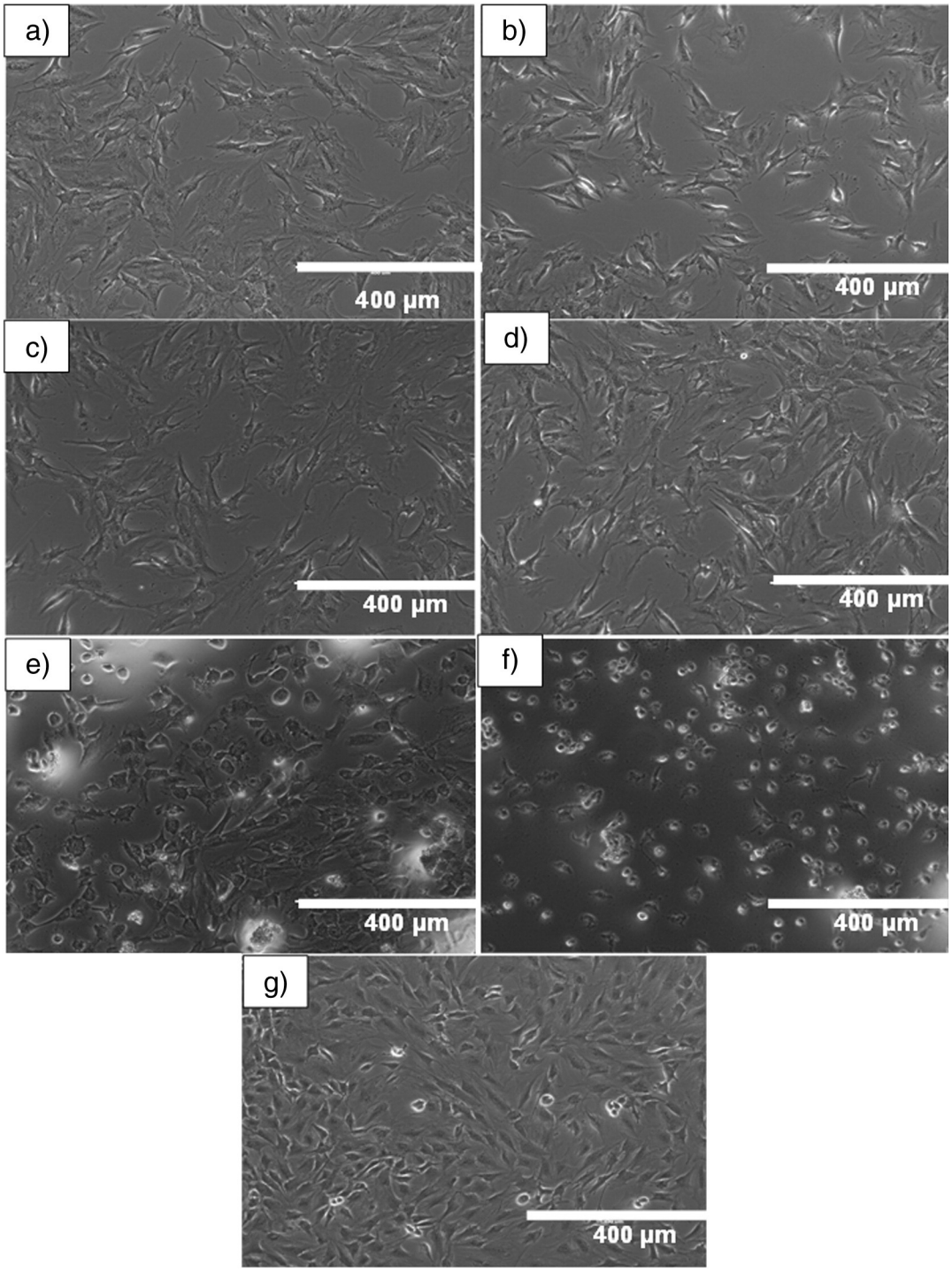

Fig. 5. Cell morphology with 12-day media collected from Mg alloys, a) AZ31 untreated, b) AZ31 anodized, c) AZ91 untreated, d) AZ91 anodized, e) ZK60 untreated, f) ZK60 anodized, g) blank control.

extracted from the potentiodynamic polarization curves via tafel fit extrapolation are summarized in Table 3. The anodization treatment has enhanced the corrosion resistance. The current densities have decreased for all three alloys. The current density for AZ31B shifted from 3.45E−05 A/cm^2 to 2.72E−06 A/cm^2, improving the corrosion rate. The same behavior was observed for the other magnesium alloys. The current density of AZ91E shifted from 3.66E−05 A/cm^2 to 2.50E−06 A/cm^2, and ZK60A current density shifted from 3.23E−05 A/cm^2 to 1.86E−06 A/cm^2. Moreover, compared to untreated magnesium alloys the E_{corr} potentials for the anodized alloys became more positive experiencing a more noble behavior. The comparison of corrosion resistance of different magnesium alloys showed a lower current density for ZK60 indicating a high corrosion resistance. High corrosion resistance of ZK60 is related to Zr element [40]. Corrosion protection of anodized ZK60 thin layer after polarization test seems more protective that other anodized layer because of the presence of zirconium oxide.

The Nyquist plots of untreated and anodized AZ31, AZ91 and ZK60 alloys were obtained in PBS solution as shown in Fig. 3. It is represented that the untreated AZ31 and AZ91 magnesium alloys showed two time constants. The first time constant at high frequency represent the activity of solution species and their interaction with the metal surface. The second distorted time constant was related to charge transfer characteristics under applied conditions. In case of AZ31 lower Z_{re} (real impedance) value (2.70 kΩ-cm^2) than AZ91 (4.85 kΩ-cm^2) corresponds to higher concentration of the dissolved metal ions initially. In case of AZ91 the decrease in impedance at low frequency corresponded to relatively high corrosion rate than AZ31 which was in support to Potentiodynamic polarization results as given in Table 3. The low Z_{re} (0.39 kΩ-cm^2) was observed for ZK60 untreated alloy representing higher dissolution of metal ions in PBS solution. The second time constant depicted lower charge transfer resistance compared to other two alloys. In anodized alloys the single time constant was obtained with a reverse Z_{re} impedance trend at low frequency. This behavior was similar for AZ31 and AZ91 but different from ZK60 as the impedance spectrum at low frequency was in the forth quadrant. This behavior was observed due to higher dissolution tendency in the electrolyte and accelerated desorption of metal cation in the electrolyte. The negative impedance in ZK60 alloy was aroused due to lower concentration polarization because of higher concentration of chlorides (reductant) ions in the electrolyte near the surface or in other words rapid oxidation of metal surface and formation of complex dissolved species in the electrolyte. The desorption of hydrogen gas could also be related with decrease in impedance at low frequency.

3.4. Percent cell viability (MTS assay) and cell morphology

In vitro tests are often performed for the evaluation of potential effects of the material on the host cells before implantation. Generally, such techniques are based and described by international standards. International standards such as ISO-10993-5 and ISO-10993-12 are commonly used by researchers to evaluate different magnesium grades [41–48]. The uses of direct and indirect methods are suggested experimental assessments for the biomaterial screening. The indirect method has been adopted. The preparation of the extracted solution samples involves immersing magnesium materials in media for a period of time. Following, the extracts are prepared making dilutions of various concentrations. In this investigation, the cell viability was studied with 100% concentrated extracted media. Fig. 4 depicts the MC3T3 cell viability cultured for 24 h with individual extraction concentrations of AZ31, AZ91, and ZK60 Mg alloys. As explained previously, media was collected every 3 days up to 21 days. The aim for this type of experiment was to monitor the magnesium degradation and the leached metal ions for a period of 21 days as seen in Fig. 3. The present results showed that the cytotoxic effect was different for the tested materials. The lowest cell viability of about 25% was observed for the ZK60 anodized alloy. Significant reduced cell viability for AZ31 and AZ91 anodized alloys could be seen during the 3-day period collected extracts. However, a recovery with steady increase in growth rate was observed for AZ91 anodized alloy for the media collected after the 6-day extracted media. AZ31 and AZ91 untreated alloys showed similar cell viability trend behavior. Overall, AZ31 and AZ91 (untreated, anodized) were less cytotoxic to the MC3T3 cells than ZK60 magnesium samples. The results also proved that the cell viability for most of the alloys was greater than 75% suggesting the cytocompatibility of AZ31, AZ91, and ZK60 [41].

Fig. 5 shows optical images of the osteoblast cells cultured for 24 h in 12-day extract media. Net cell growth is related to the MTS plotted data. The results demonstrated good cell morphology for the extracted media from AZ31 and AZ91 untreated and anodized alloys, however the cell growth in the ZK60 extracted media does not show a good cell morphology and proliferation when compared with the control.

4. Conclusions

AZ31B, AZ91E and ZK60A alloys were investigated as potential biodegradable orthopedic implant materials. The SEM analysis showed that the alloys' morphology was completely changed depicting microtextured features formed after the anodization chemical treatment. For the wettability studies, the anodic treatment made the surfaces behave more hydrophobic. Also, the surface free energy was decreased for the anodized materials. The electrochemical experiments demonstrated that the corrosion rate improved for AZ31B, AZ91E, and ZK60A anodized materials as compared to the untreated surfaces. Ultimately, the in vitro analysis by indirect MTS assay displayed lowest cell viability of 25% for ZK60 anodized. Significant reduced cell viability was observed between days 3 and 9 for the extracted media of AZ31 and AZ91 alloys. The cell viability was greater than 75% implying the cytocompatibility of the magnesium alloys. However, challenges in biomedical evaluations consist of several trials to establish the long-term biocompatibility of magnesium based alloys and their corrosion products within the body; therefore further biocompatibility studies should still be performed.

References

[1] N.J. Ostrowski, B. Lee, A. Roy, M. Ramanathan, P.N. Kumta, Biodegradable poly(lactide-co-glycolide) coatings on magnesium alloys for orthopedic applications, J. Mater. Sci. Mater. Med. 24 (1) (2012) 85–96.
[2] M.P. Staiger, A.M. Pietak, J. Huadmai, G. Dias, Magnesium and its alloys as orthopedic biomaterials: a review, Biomaterials 27 (2006) 1728–1734.
[3] K. Hanada, K. Matsuzaki, X. Huang, Y. Chino, Fabrication of Mg alloy tubes for biodegradable stent application, Mater Sci Eng C Mater Biol Appl, 33(8), Elsevier B.V., Dec 1 2013, pp. 4746–4750.
[4] M. Salahshoor, Y. Guo, Biodegradable orthopedic magnesium–calcium (MgCa) alloys, processing, and corrosion performance, Materials (Basel) 5 (12) (Jan 9 2012) 135–155.
[5] F. Witte, H. Ulrich, M. Rudert, E. Willbold, Biodegradable magnesium scaffolds: part 1: appropriate inflammatory response, J. Biomed. Mater. Res. A 81 (2007) 748–756.
[6] F. Witte, H. Ulrich, C. Palm, E. Willbold, Biodegradable magnesium scaffolds: part II: peri-implant bone remodeling, J. Biomed. Mater. Res. A 81 (2007) 757–765.
[7] H. Windhagen, K. Radtke, A. Weizbauer, J. Diekmann, Y. Noll, U. Kreimeyer, et al., Biodegradable magnesium-based screw clinically equivalent to titanium screw in hallux valgus surgery: short term results of the first prospective, randomized, controlled clinical pilot study, Biomed. Eng. Online 12 (1) (Jan 2013) 62.
[8] G. Wu, J.M. Ibrahim, P.K. Chu, Surface design of biodegradable magnesium alloys — a review, Surf Coatings Technol [Internet], 233, Elsevier B.V., Oct 2013, pp. 2–12.
[9] S. Chen, S. Guan, W. Li, H. Wang, J. Chen, Y. Wang, et al., In vivo degradation and bone response of a composite coating on Mg–Zn–Ca alloy prepared by microarc oxidation and electrochemical deposition, J. Biomed. Mater. Res. B Appl. Biomater. (2011) 533–543.
[10] A. Hartwig, Role of magnesium in genomic stability, Mutation Research — Fundamental and Molecular Mechanisms of Mutagenesis2001. 113–121.
[11] Y.W. Song, D.Y. Shan, E.H. Han, Electrodeposition of hydroxyapatite coating on AZ91D magnesium alloy for biomaterial application, Mater. Lett. 62 (2008) 3276–3279.
[12] C. Lhotka, T. Szekeres, I. Steffan, K. Zhuber, K. Zweym, Four-year study of cobalt and chromium blood levels in patients managed with two different metal-on-metal total hip replacements, 21 (2003) 189–195.
[13] J.J. Jacobs, N.J. Hallab, A.K. Skipor, R.M. Urban, Metal degradation products: a cause for concern in metal-metal bearings? Clin. Orthop. Relat. Res. (2003) 139–147.

[14] D. Granchi, G. Ciapetti, S. Stea, L. Savarino, F. Filippini, A. Sudanese, et al., Cytokine release in mononuclear cells of patients with Co–Cr hip prosthesis, 20 (1999) 1079–1086.
[15] Y. Niki, H. Matsumoto, Y. Suda, T. Otani, K. Fujikawa, Y. Toyama, et al., Metal ions induce bone-resorbing cytokine production through the redox pathway in synoviocytes and bone marrow macrophages, Biomaterials 24 (8) (Apr 2003) 1447–1457.
[16] H. Waizy, J.-M. Seitz, J. Reifenrath, A. Weizbauer, F.-W. Bach, A. Meyer-Lindenberg, et al., Biodegradable magnesium implants for orthopedic applications, J. Mater. Sci. 48 (1) (May 24 2012) 39–50 (cited 2014 Jul 16).
[17] R. Xu, X. Yang, K.W. Suen, G. Wu, P. Li, P.K. Chu, Applied surface science improved corrosion resistance on biodegradable magnesium by zinc and aluminum ion implantation atomic concentration (%), 263 (2012) 608–612.
[18] Y. Xin, C. Liu, X. Zhang, G. Tang, X. Tian, P.K. Chu, Corrosion behavior of biomedical AZ91 magnesium alloy in simulated body fluids, J. of Mat. Res. 2 (07) (2007) 2004–2011.
[19] C. Liu, Y. Xin, G. Tang, P.K. Chu, Influence of heat treatment on degradation behavior of bio-degradable die-cast AZ63 magnesium alloy in simulated body fluid, Mater. Sci. Eng. A 456 (2007) 350–357.
[20] F. Witte, J. Fischer, J. Nellesen, H.-A. Crostack, V. Kaese, A. Pisch, et al., In vitro and in vivo corrosion measurements of magnesium alloys, Biomaterials 27 (7) (Mar 2006) 1013–1018.
[21] L. Li, J. Gao, Y. Wang, Evaluation of cyto-toxicity and corrosion behavior of alkali-heat-treated magnesium in simulated body fluid, Surf. Coat. Technol. 185 (2004) 92–98.
[22] C. Liu, Y. Xin, X. Tian, P.K. Chu, Corrosion behavior of AZ91 magnesium alloy treated by plasma immersion ion implantation and deposition in artificial physiological fluids, Thin Solid Films 516 (2007) 422–427.
[23] F. Witte, V. Kaese, H. Haferkamp, E. Switzer, A. Meyer-Lindenberg, C.J. Wirth, et al., In vivo corrosion of four magnesium alloys and the associated bone response, Biomaterials 26 (17) (Jun 2005) 3557–3563.
[24] F. Sanling, L. Quanan, J. Xiaotian, Z. Qing, C. Zhi, L. Wenjian, Review on research and development of heat resistant Magnesium alloy, Proceedings of 2012 International Conference on Mechanical Engineering and Material Science (MEMS 2012), 2012 http://dx.doi.org/10.2991/mems.2012.179.
[25] C.J. Boehlert, K. Knittel, The microstructure, tensile properties, and creep behavior of Mg–Zn alloys containing 0–4.4 wt.% Zn, Mater. Sci. Eng. A 417 (1–2) (Feb 2006) 315–321.
[26] N. Angrisani, J. Seitz, A. Meyer-Lindenberg, J. Reifenrath, Rare earth metals as alloying components in magnesium implants for orthopaedic applications, in: Waldemar A Monteiro (Ed.) New Features on Magnesium Alloys, InTech, 2012 http://dx.doi.org/10.5772/48335 (ISBN: 978-953-51-0668-5).
[27] J. Wang, J. Tang, P. Zhang, Y. Li, J. Wang, Y. Lai, et al., Surface modification of magnesium alloys developed for bioabsorbable orthopedic implants: a general review, J. Biomed. Mater. Res. B Appl. Biomater. 100 (6) (Aug 2012) 1691–1701.
[28] G. Eddy Jai Poinern, S. Brundavanam, D. Fawcett, Biomedical magnesium alloys: a review of material properties, surface modifications and potential as a biodegradable orthopaedic implant, Am. J. Biomed. Eng. 2 (6) (Jan 7 2013) 218–240.
[29] N. Nassif, I. Ghayad, Corrosion protection and surface treatment of magnesium alloys used for orthopedic applications, Adv. Mater. Sci. Eng. 2013 (2013) 10 http://dx.doi.org/10.1155/2013/532896 (Article ID 532896).
[30] M. Hara, K. Matsuda, W. Yamauchi, M. Sakaguchi, T. Yoshikata, Y. Takigawa, et al., Optimization of environmentally friendly anodic oxide film for magnesium alloys, Mater. Trans. 47 (4) (2006) 1013–1019.
[31] Stephen Abela, Protective coatings for magnesium alloys, in: Frank Czerwinski (Ed.)Magnesium Alloys — Corrosion and Surface Treatments, ISBN: 978-953-307-972-1, 2011.
[32] ASTM G102-89, Standard practice for calculation of corrosion rates and related information from electrochemical measurements, Annual Book of ASTM Standards2010. 1–7.
[33] C. Blawert, W. Dietzel, E. Ghali, G. Song, Anodizing treatments for magnesium alloys and their effect on corrosion resistance in various environments, Adv. Eng. Mater. 8 (2006) 511–533.
[34] S. Salman, R. Mori, R. Ichino, M. Okido, Effect of anodizing potential on the surface morphology and corrosion property of AZ31 magnesium alloy, Mater. Trans. 51 (6) (2010) 1109–1113.
[35] H. Lan Wu, Y. Liang Cheng, L. Ling Li, Z. Hua Chen, H. Min Wang, Z. Zhang, The anodization of ZK60 magnesium alloy in alkaline solution containing silicate and the corrosion properties of the anodized films, Appl. Surf. Sci. 253 (2007) 9387–9394.
[36] Y. Mizutani, S.J. Kim, R. Ichino, M. Okido, Anodizing of Mg alloys in alkaline solutions, Surf. Coat. Technol. 169–170 (2003) 143–146.
[37] N.A. El Mahallawy, AZ91 magnesium alloys: anodizing of using environmental friendly electrolytes, J. Surf. Eng. Mater. Adv. Technol. 01 (02) (2011) 62–72.
[38] W.R. Lacefield, Materials characteristics of uncoated/ceramic-coated implant materials, Adv. Dent. Res. 13 (1999) 21–26.
[39] R.B. Parekh, O. Shetty, R. Tabassum, Surface modifications for endosseous dental implants, in: L. Mahesh (Ed.)Int J Oral Implantol Clin Res, 3, Sep 15 2012, pp. 116–121.
[40] Y. Liang Cheng, T. Wei Qin, H. Min Wang, Z. Zhang, Comparison of corrosion behaviors of AZ31, AZ91, AM60 and ZK60 magnesium alloys, Trans. Nonferrous Met. Soc. China 19 (2009) 517–524.
[41] J. Fischer, D. Pröfrock, N. Hort, R. Willumeit, F. Feyerabend, Improved cytotoxicity testing of magnesium materials, Mater Sci Eng B, 176(11), Elsevier B.V., Jun 2011, pp. 830–834.
[42] Y. Sun, M.X. Kong, X.H. Jiao, In-vitro evaluation of Mg–4.0Zn–0.2Ca alloy for biomedical application, Trans. Nonferrous Met. Soc. China 21 (2011).
[43] J. Niu, G. Yuan, Y. Liao, L. Mao, J. Zhang, Y. Wang, et al., Enhanced biocorrosion resistance and biocompatibility of degradable Mg–Nd–Zn–Zr alloy by brushite coating, Mater. Sci. Eng. C 33 (2013) 4833–4841.
[44] X. Gu, Y. Zheng, Y. Cheng, S. Zhong, T. Xi, In vitro corrosion and biocompatibility of binary magnesium alloys, Biomaterials 30 (2009) 484–498.
[45] P. Gill, N. Munroe, R. Dua, S. Ramaswamy, Corrosion and biocompatibility assessment of magnesium alloys, J. Biomater. Nanobiotechnol. 3 (1) (2012) 10–13.
[46] Z.G. Huan, M.A. Leeflang, J. Zhou, L.E. Fratila-Apachitei, J. Duszczyk, In vitro degradation behavior and cytocompatibility of Mg–Zn–Zr alloys, J. Mater. Sci. Mater. Med. 21 (2010) 2623–2635.
[47] D. Hong, P. Saha, D.-T. Chou, B. Lee, B.E. Collins, Z. Tan, et al., In vitro degradation and cytotoxicity response of Mg–4% Zn–0.5% Zr (ZK40) alloy as a potential biodegradable material, Acta Biomater, 9(10), Acta Materialia Inc., Nov 2013, pp. 8534–8547.
[48] S. Guan, J. Hu, L. Wang, S. Zhu, H. Wang, J. Wang, et al., Mg Alloys Development and Surface Modification for Biomedical Application, 2007.